Raman spectra of silver-halide melts and sublattice melting in the superionic conductor α-AgI†

M. J. Delaney and S. Ushioda
Department of Physics, University of California at Irvine, Irvine, California 92717
(Received 23 February 1977)

We have measured the Raman spectra of AgBr and AgCl in both the high-temperature solid and the melt. The melt spectra are strikingly similar to the spectrum of the superionic conductor α-AgI. We have found that second-order Raman scattering from short-wavelength vibrations ("zone-boundary" phonons) is the primary scattering mechanism for the melts. The α-AgI spectrum coincides with the silver-halide melt spectra when frequency is scaled by inverse square root of the halide mass ratio. We believe that the α-AgI spectrum is also due mainly to the second-order processes and is affected by the molten cation sublattice. We find no evidence for a direct connection between the cation motion in α-AgI and the Raman spectrum.

I. INTRODUCTION

Recently, we have reported the Raman spectra of the superionic conductors AgI and $RbAg_4I_5$.[1] In that work and the work of other authors[2] on the subject, there has been a degree of uncertainty as to the origin of the observed spectra. We have pursued our present work in related materials in an attempt to clarify some of the unanswered questions concerning superionic conductors.

Silver iodide is known as one of the classic superionic conductors. Many articles describing its physical properties have appeared in the past.[3] At 147 °C there is a phase transition from normal (β phase) to superionic state. In this high-temperature α phase there is a cation conductivity many orders of magnitude higher than in ordinary crystalline solids. The Raman spectrum undergoes dramatic changes at the transition to this superionic state, which is accompanied by a structural phase transition. Our first interest in these materials was prompted by the hope of determining the dynamics of cation motion from studies of the Raman spectra. The Raman spectrum of α-AgI is very interesting in that for a crystalline material its features are very broad and structureless. It decreases almost exponentially from low energies near the laser line out to 200 cm^{-1} with only a weak shoulder at 100 cm^{-1}. There are many suggested origins for this spectrum and we shall discuss them in detail later. We have come to the conclusion that previous explanations are not adequate.

We have decided to take a different approach. The nature of the $\beta \rightarrow \alpha$ transition, with the cations becoming highly mobile, gives one a picture of sublattice melting upon entering the superionic phase. Supporting this physical picture is the fact that the ionic conductivity of α-AgI just above the $\beta \rightarrow \alpha$ transition is comparable to that in ionic melts; AgBr and AgCl have ionic conductivities in the melt of 2.9 and 3.7 $(\Omega\,cm)^{-1}$, respectively. An interesting point is that while the conductivity of AgI increases from 1.3 to 2.5 $(\Omega\,cm)^{-1}$ in the superionic phase, it drops to 2.38 $(\Omega\,cm)^{-1}$ upon melting.[4] It has also been found that the change in entropy of AgI at the $\beta \rightarrow \alpha$ transition (3.48 cal/mole K) is greater than at melting (2.7 cal/mole K) and comparable to the change of entropy at melting of AgCl and AgBr, 3.11 and 4.23 cal/mole K, respectively.[5] It is this liquidlike behavior of α-AgI that prompted us to examine the Raman spectra of ionic melts. We chose AgBr and AgCl because of their low melting points, 434 °C and 455 °C, respectively. We also felt that it would be easier to compare these silver halides to α-AgI.

We have found the Raman spectra of these silver-halide melts strikingly similar to the spectrum of α-AgI. A discussion of the melt spectra in terms of second-order scattering processes is dealt with in detail. We have analyzed our spectra in this regard and believe that our results will further support the picture of sublattice melting in α-AgI.

In Sec. II the sample preparation and experimental procedures are described. Section III deals with AgI; its properties, the Raman spectrum, and its proposed origins. In Sec. IV we describe our results from the silver-halide melts, the nature of the scattering and the relationship to α-AgI.

II. EXPERIMENTAL

The preparation and experimental procedures used to obtain the Raman spectrum of AgI are reported elsewhere.[1] Samples of AgBr and AgCl to be melted were sealed in evacuated Pyrex tubes. Crystalline samples obtained from Harshaw were cut into rectangular parallelopipeds of dimensions $5 \times 2 \times 10$ mm and polished. Suitable precautions had to be taken in mounting these silver-halide samples due to reactions and decomposition when

in contact with metals. Alumina holders were devised for these samples. The samples were mounted in an evacuated oven with temperature controlled to ±1 °C. A 90° scattering geometry was employed with the 6328-Å line of a He-Ne laser as the exciting source. Laser power was limited to 10 mW defocused, in order to prevent surface damage to the solid samples. The scattered light was analyzed by a Spex 1400 double grating spectrometer and a cooled ITT-FW130 photomultiplier using a computer-controlled photon counting system.[6] Low-temperature measurements were made at nitrogen temperature using a standard Dewar system and a 5145-Å argon laser line as the exciting source. Difficulties with luminescence as described by Van der Osten[7] were encountered. However with repeated scans of our computer-controlled system we were able to subtract this large background and combine the resulting spectra to improve the signal-to-noise ratio.

We note here that attempts to obtain the spectra of molten AgI failed. AgI in the melt is not transparent to the 6328-Å laser line and attempts at backscattering failed due to a large amount of scattering from the quartz container.

III. RESULTS AND DISCUSSION: AgI

Below 147 °C silver iodide is a "normal" crystal with the wurtzite structure having well defined phonon peaks in the Raman spectrum. At 147 °C it undergoes a first-order phase transition to its superionic state where the structure changes from wurtzite to a body-centered-cubic iodine lattice with several possible sites within the new unit cell for each silver ion. It is this large number of silver sites created by the iodine lattice with low activation energies (0.1 eV as determined from diffusion measurements[8]) that gives the large mobility for the silver ions. This together with the large number of mobile cations gives the large conductivity for which these materials are known.

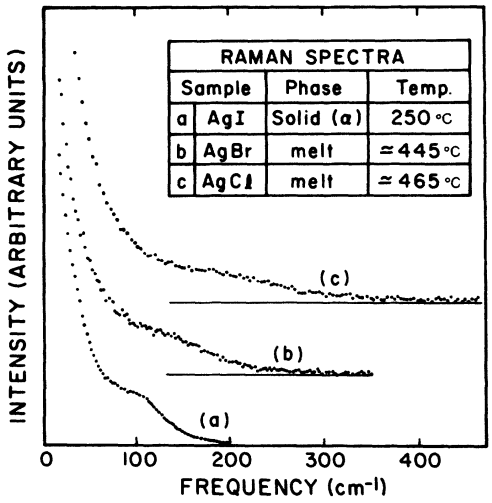

FIG. 1. Raman spectra of (a) the superionic conductor α-AgI, (b) the silver-bromide melt, and (c) the silver-chloride melt. The background has been subtracted from these spectra. The zero of intensity has been shifted for (b) and (c).

As mentioned previously, the Raman spectrum of α-AgI is quite striking. We observe, in Fig. 1(a), very intense low-energy scattering that drops off sharply, almost exponentially, to a very broad shoulder around 100 cm^{-1} and then tails off slowly to approximately 200 cm^{-1}. This spectral shape is observed from the onset of the superionic state at 147 °C to near melting. The broad and relatively featureless nature of the spectra and the lack of any theory of Raman scattering for superionic conductors have made a detailed analysis of the data extremely difficult. In the wurtzite structure the first- and second-order Raman spectra are well understood and a majority of the scattering takes place in the 80–120-cm^{-1} region. The region contains A_1, E_1, and E_2 symmetry optical phonons at $k \simeq 0$, along with a broad second-order feature. Above the phase transition there is a large increase in the low-frequency scattering; it is this low-frequency scattering that dominates the spectrum in Fig. 1(a). The fact that this sudden increase in scattering coincides with the anomalous jump in the ionic conductivity has caused the features in this low-frequency region to be associated with the motion of the cations. One must also recall that the onset of low-frequency scattering coincides with a structural phase transition. When considering the origin of this scattering in the low-frequency region it is important to take into account the Bose-Einstein thermal population factor. The presence of this factor, which varies approximately inversely with frequency, will distort the spectral density function of the low-energy excitations. As shown in our previous work,[1] dividing this Bose-Einstein factor out of the spectrum of α-AgI gives a maximum in the spectral density away from zero frequency (this point will be discussed later). The broad shoulder at 100 cm^{-1} is thought to be reminiscent of the $k \simeq 0$ optical-phonon modes in the wurtzite phase. Across the $\beta \rightarrow \alpha$ phase transition, the scattering intensity of this region remains approximately constant. In the wurtzite phase the Ag^+ sits at the center of an iodine tetrahedron with a Ag-I distance of 2.81 Å. In α-AgI with space group O_h^9-$Im3m$ it is thought[9] that the cation is at a d site which is at the center of an iodine tetrahedron with Ag-I distance of 2.87 Å.

$RbAg_4I_5$ which has a much narrower peak at 108 cm^{-1} in its Raman spectra also has the Ag^+ at the center of an iodine tetrahedron with Ag-I distance of approximately 2.85 Å.[10] It has been suggested that this peak is due to the breathing mode of the iodine tetrahedron.[11] These similarities in structure lead us to believe that the high energy end of the α-AgI spectra is due to lattice phonon modes. Standard temperature-dependence analysis of the spectra has proved inconclusive due to the rapid narrowing of the optical gap with increasing temperature.

With the above analysis the following questions still remain. If the low-frequency feature is due to cation motion, what is the light-scattering mechanism? Does it reflect the distribution of hopping frequencies, an attempt frequency for hopping, scattering from density fluctuations caused by cation motion, or is it in fact due to the cation motion at all? Concerning the proposed phonon structure of α-AgI, some fraction of the cations could occupy b-, h-, or g-type sites giving different vibrational structures. The broad structureless nature of this region indicates that a single first-order phonon picture may not be appropriate. The disorder in the system removes $k \cong 0$ selection rule and we could be observing the one- or two-phonon density of states. In short, there are many possible explanations but exact conclusions cannot be drawn from existing data, without the support of a detailed theory.

IV. RESULTS AND DISCUSSION: AgBr AND AgCl

In Figs. 1(b) and 1(c) we show the Raman spectra of molten AgBr and AgCl. We see that the spectral shape is very similar to that of α-AgI. The melt spectra have strong low-energy scattering with a weak shoulder at higher frequencies. The spectra show no other structure. The extension of the AgCl spectrum to energies higher than AgBr is expected, chlorine having a smaller mass than bromine. Current experiments are limited to temperatures just above melting of these silver halides. We found that these spectra were independent of scattering angle and have depolarization ratio of approximately one.

We now wish to understand the meaning of this remarkable resemblance of the spectra of α-AgI and the silver-halide melt. An understanding of the melt spectra should help in determining the nature of the Raman scattering in superionic conductors. We thus turn to a discussion of the Raman spectra of these silver-halide melts. Above the melting point we would expect that the nearest-neighbor environment for the ions in the melt resembles that in the solid phase. A cation is surrounded by a number of anions at an average distance which is not radically different from that in the solid. In such a system there is no longer any long-range order. There still is short-range order that allows the existence of short-wavelength vibrations, reminiscent of zone-boundary phonons of the solid phase, in the liquid. In the solid phase AgBr and AgCl have NaCl structure at all temperatures. Because these crystals have a center of inversion at each atomic site, first-order Raman processes are forbidden. The observed spectra in solid AgBr and AgCl are completely second order in nature. The second-order spectra at room temperature and liquid-nitrogen temperature have been reported by several authors.[7,12] The large number of overlapping combinations and overtones from different points in the Brillouin zone have made identification of the structure in the spectra extremely difficult. Polarization studies at low temperatures and neutron data have not resolved this problem. The spectrum of AgBr at 20 °C, Fig. 2(a), has one prominent feature at 80 cm^{-1} with a shoulder at higher frequencies. As temperature increases the structure broadens out and the spectrum becomes smooth. Figure 2(c) is the second-order spectrum at 360 °C. The low-frequency region below 100 cm^{-1} has rapidly grown in intensity and the peak in Fig. 2(a) is now a faint shoulder. Spectra of these samples were taken at nitrogen temperature and found to coincide with data obtained by Van der Osten.[7] This was done to verify the orientation and purity of our samples and to find if the low-energy scattering was removed with reduced temperature. The high-intensity low-energy scattering is strongly affected by the presence of the Bose-Einstein thermal popula-

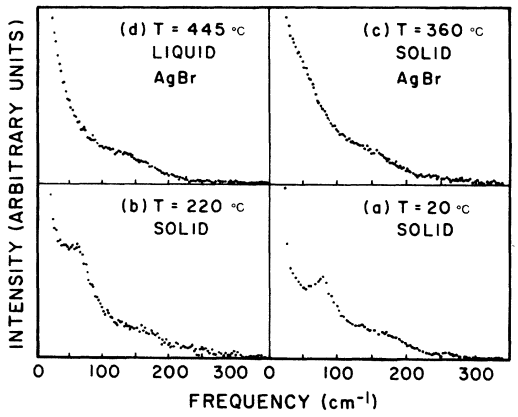

FIG. 2. Raman spectra of silver bromide in both solid and molten phase. The background has been subtracted and the intensity adjusted to show the region of the low-frequency structure. This structure is attributed to combinations of zone-boundary acoustic phonons.

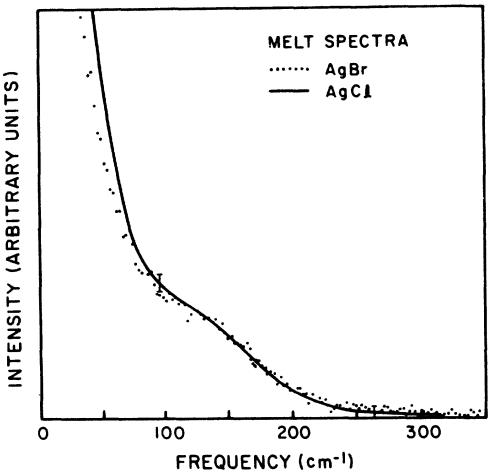

FIG. 3. Raman spectrum of molten AgBr (solid circles are actual data points) is compared with the scaled spectrum of molten AgCl (solid line). We have drawn a solid line through the AgCl data points to facilitate the comparison. (Error bars indicate spread of AgCl data.) The silver chloride frequency axis has been scaled by the inverse square root of the halide mass ratio. The intensity has been scaled for a best fit.

tion factors. It is well known that second-order Stokes scattering increases rapidly with increasing temperature, especially at low energies. The second-order Bose-Einstein factor varies approximately as T^2/ω^2. Of particular interest is the relation of the high-temperature solid spectrum of silver bromide to the melt spectrum. The spectra are very similar although we do observe that the high-temperature solid still has some structure, whereas the melt spectrum is completely smooth. Although this comparison is surprising, it is not completely new; Barker[13] has found that the multiphonon infrared absorption of alkali halides is not changed by melting. Fleury *et al.*[14] found that the second-order Raman spectrum of Xe, Kr, and Ar did not change appreciably upon melting. With these examples we feel confident that the melt spectra are due to second-order processes.

We had initially thought that the strong low-frequency scattering at higher temperatures might be due to the large increase in Frenkel defects, which reach a few percent near melting. The large number of interstitials, with mobilities comparable to the cations in superionic conductors, give these silver halides ionic conductivities on the order of 0.1 $(\Omega\,\mathrm{cm})^{-1}$ at elevated temperatures. It was thought that one might observe extra scattering at low frequency due to the hopping motion of the cations, as well as attempt frequencies, between lattice sites and interstitials. This type of scattering has been hypothesized for superionic conductors. Such a process would have a strong temperature dependence due to the thermal activation of these defects.

We also expect the possibility of observing defect induced first-order scattering[15] which would allow us to observe the one-phonon density of states. We would also expect this to increase with temperature as the number of interstitials reduce the symmetry of the crystal. The one-phonon density of states will, in general, have broad features although the zone-center optical-phonon peaks should stand out. This contribution would be added onto the broad two-phonon features. One difficulty in observing this is that the defect-induced first-order scattering will be strongest only at the higher temperatures where the second-order scattering is dominant.

We have compared the AgBr solid spectra at various temperatures and currently there does not appear to be any excess scattering at higher temperatures. However we note that this analysis is difficult due to poor statistics at higher frequencies originating from weak scattering and the difficulties in comparing spectra of different temperatures. At present a 10% effect on top of the second-order spectra may go unnoticed.

In Fig. 3, we compare the spectra of the silver bromide and silver chloride melts. These spectra were taken at similar temperatures (just above melting) and we believe that both spectra are due to second-order scattering from zone boundary phonons. These spectra should be very similar except for the extension of AgCl spectrum to higher frequencies due to smaller chlorine mass. Using simple mass scaling of the frequency axis we find that scaling the AgCl spectrum by inverse square root of the halide mass ratio (0.666) gives excellent agreement above 80 cm^{-1}. We have actually scaled by 0.68 and adjusted the intensity for a best fit. Scaling by inverse square root of the halide mass ratio agrees with the experimental value far better than the inverse square root of the ratio of reduced masses (0.762). In a simple picture the frequency scales with the inverse square root of the halide mass for phonons at the edge of the Brillouin zone. There is a discrepancy between the melt spectra below 80 cm^{-1}. We have no explanation for this other than to say that with such a simple scaling scheme one should not be surprised by small differences.

We recall the close resemblance of the α-AgI and the silver-halide melt spectra. In Fig. 4 we compare the spectra of molten AgCl and solid α-AgI. Assuming the similar processes are responsible for scattering in both materials, we rescale the silver chloride frequency axis. In this case

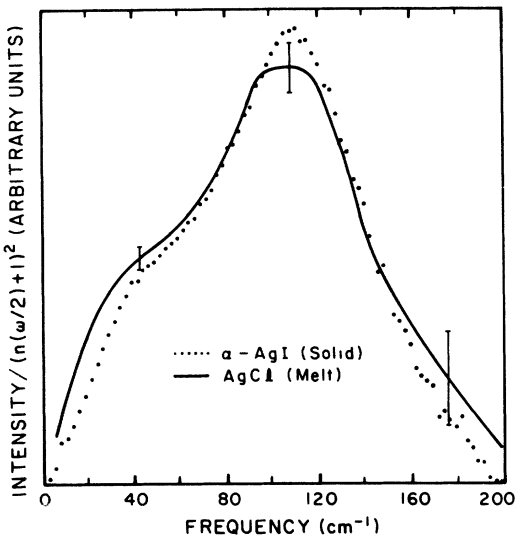

FIG. 4. Raman spectrum of the superionic conductor α-AgI at 250 °C (solid circles) is compared with the spectrum of the AgCl melt at 465 °C. Both spectra have the second-order thermal factors $[n(\frac{1}{2}\omega)+1]^2$ divided out (see text). The error bars indicate the spread in the silver chloride data. The silver chloride frequency axis has been scaled by the inverse square root of the halide mass ratio. The intensity has been scaled for a best fit.

because of the large differences in temperature 250 (α-AgI) and 465 °C (AgCl), we compare the spectra with the second-order thermal factor $[n(\frac{1}{2}\omega)+1]^2$ divided out. The Raman intensity is divided by $[n(\frac{1}{2}\omega)+1]^2$ at every point, where $n(\omega)$ is the Bose-Einstein population factor. This is a good first approximation for the whole spectrum even though it is not made up entirely of overtones. For second-order processes the thermal occupation number is made up of the products of the two Bose-Einstein factors for the phonons involved; i.e., $[n(\omega_1)+1][n(\omega_2)+1]$ for a combination process involving two phonons of frequencies ω_1 and ω_2. For fixed frequency, the relative change in occupation number with temperature is approximately the same for all processes even though the absolute magnitudes are different. A frequency scaling factor of 0.51 is found for the best fit. The inverse square root of the halide mass ratio in this case is 0.528. We do not believe that this is coincidental. This comparison tells us that the α-AgI spectrum is due primarily to second-order processes similar to that of the silver-halide melts. It also indicates that the same types of processes occur in both substances and in this frequency region the two systems look alike. Comparison to other phases of AgI show that interpretation in terms of second-order scattering is appropriate. The high-pressure rocksalt phase of AgI,[2] which only has second-order scattering in the Raman spectrum, has the same frequency extent as α-AgI and in fact scales nicely with the solid AgBr and AgCl spectra. In addition, the high-pressure tetragonal phase of AgI has its first-order Raman structure below 115 cm^{-1}. A question arises as to the actual structural differences of the different phases of these materials. α-AgI has a proposed tetrahedrally coordinated cation site with Ag-I distances of 2.87 Å, whereas in the solid phase AgCl and AgBr have Ag-halide distances of 2.87 and 2.89 Å, respectively. The cations in the NaCl structure, however, have six nearest neighbors. Currently there is no neutron or x-ray data giving the nearest-neighbor distances for the silver-halide melts. There are neutron data on alkali-halide melts and it has been found that, in general, there is only a few percent reduction in cation-anion distances upon melting. The number of nearest neighbors, on the other hand, drops from 6 to 4 or 5. If, in actuality, this also occurs in the silver halides upon melting, it is not readily evident in the Raman spectra we have observed. It is therefore not clear how much this apparent structural difference will affect the second-order Raman spectra of these silver halides in their different high-temperature solid and molten phases.

We now turn our attention to the hypothesis that we are observing the effect of a molten cation sublattice in superionic AgI. Recall, as we stated above, that upon melting the only change in the AgBr spectrum was the loss of the remaining small structure at low frequencies and that other than that change the spectra were identical. We believe that this is an important distinction between the two spectra. The distinction between the solid and the melt is the loss of long-range order and the consequent broadening of the distinct vibrational structure in the melt spectrum. The α-AgI spectrum does not have any of the sharp structure one would expect from second order scattering in a solid. In fact whereas the spectral structure in AgBr changes considerably with temperature, the shape of the AgI spectrum remains essentially constant in the α phase. This indicates that superionic AgI is, with regard to Raman scattering, molten. α-AgI no longer has the long-range order of a solid; it has the vibrational structure of a liquid.

V. CONCLUSIONS

We have found that the superionic conductor α-AgI behaves as though it has melted in its high-temperature solid phase. That is, the Raman

spectrum of α-AgI is very similar in shape to the Raman spectra of the AgBr and AgCl melts. We believe that these melt spectra are due to second-order Raman scattering from short-wavelength vibrations. This conclusion is a result of following the temperature dependence of the second-order spectra in AgBr up to melting. There does not appear to be any scattering due to thermally induced Frenkel defects in the solid at high temperatures. There are only minor but important changes in the spectrum upon melting. Using simple frequency-scaling techniques we have found that the AgBr and the AgCl melt spectra are nearly identical when scaled by inverse square root of the halide mass ratio. Using this method we found that the solid α-AgI spectrum is very similar to the melt spectrum of AgCl when thermal factors have been removed. These comparisons indicate that the α-AgI spectrum is mainly due to second-order Raman processes involving short-wavelength vibrations. We believe that the lack of structure in the α-AgI spectrum and its close relationship to the melt spectra of AgCl and AgBr indicates that there has been a cation sublattice melting at the $\beta \rightarrow \alpha$ transition. We have not observed the attempt or hopping frequencies for cation motion between sublattice sites or the low-frequency collisional scattering of Ref. 14 as was initially expected in the Raman spectra of superionic conductors.

ACKNOWLEDGMENTS

We thank D. L. Mills and K. R. Subbaswamy for useful discussions during the course of this work.

---

†Research supported by NSF under Grant No. DMR 73-02486-A02.

[1]M. J. Delaney and S. Ushioda, Solid State Commun. 19, 297 (1976).

[2]R. C. Hanson, T. A. Fjeldly, and H. D. Hochheimer, Phys. Status Solidi B 70, 567 (1975); G. Burns, F. H. Dacol, and M. W. Shafer, Solid State Commun. 19, 291 (1976).

[3](a) See *Superionic Conductors*, edited by G. D. Mahan and W. L. Roth (Plenum, New York, 1976); and (b) *Fast Ion Transport in Solids, Solid State Batteries and Devices*, edited by W. Van Gool (North-Holland, Amsterdam, 1973).

[4]A. Kvist and A. M. Josefson, Z. Naturforsch 23A, 625 (1968).

[5]*American Institute of Physics Handbook*, edited by D. E. Gray (McGraw-Hill, New York, 1963), pp. 4–172.

[6]S. Ushioda, J. B. Valdez, W. H. Ward, and A. R. Evans, Rev. Sci. Instrum. 45, 479 (1974).

[7]W. van der Osten, Phys. Rev. B 9, 789 (1974).

[8]A. Kvist and R. Tärneberg, Z. Naturforsch 25A, 257 (1970).

[9]See S. Geller, in Refs. 3(a) and 3(b).

[10]S. Geller, Science 157, 310 (1967).

[11]D. Gallagher and M. V. Klein, J. Phys. C 9, L687 (1976).

[12]G. L. Bottger and C. V. Damsgard, Solid State Commun. 9, 1277 (1971).

[13]A. J. Barker, J. Phys. C 5, 2276 (1972).

[14]P. A. Fleury, J. M. Worlock, and H. L. Carter, Phys. Rev. Lett. 30, 591 (1973).

[15]S. Ushioda, Solid State Commun. 15, 149 (1974).